Carbohydrate Research 361 (2012) 33–40

Contents lists available at SciVerse ScienceDirect

Carbohydrate Research

journal homepage: www.elsevier.com/locate/carres

Glycosylation of N^{α}-lauryl-*O*-(β-D-xylopyranosyl)-L-serinamide as a saccharide primer in cells

Yinan Wang [a], Tomoaki Kumazawa [a], Keisuke Shiba [a], Kenji Osumi [b], Mamoru Mizuno [b], Toshinori Sato [a,*]

[a] Department of Biosciences and Informatics, Keio University, Hiyoshi, Yokohama 223-8522, Japan
[b] Laboratory of Glyco-organic Chemistry, The Noguchi Institute, Kaga 1-8-1, Itabashi-Ku, Tokyo 173-0003, Japan

ARTICLE INFO

Article history:
Received 2 July 2012
Received in revised form 8 August 2012
Accepted 9 August 2012
Available online 17 August 2012

Keywords:
Glycosaminoglycan
Saccharide primer
Oligosaccharide
FBJ osteosarcoma

ABSTRACT

N^{α}-Lauryl-*O*-(β-D-xylopyranosyl)-L-serinamide (Xyl-Ser-C12) was synthesized as a saccharide primer to obtain oligosaccharides of glycosaminoglycan using the glycan biosynthetic potential of mouse osteosarcoma FBJ-S1 cells and Chinese hamster ovary (CHO) cells. The glycosylated products secreted into the culture medium were collected and analyzed by liquid chromatography–mass spectrometry and glycosidase digestion. The structure of the Xyl-Ser-C12 derivatives was investigated. Several glycosaminoglycan-type oligosaccharides, such as GalNAc-(GlcA-GlcNAc)$_n$-GlcA-Gal-Gal-Xyl-Ser-C12, were detected, and identified as intermediates of the biosynthesis of heparan sulfate glycosaminoglycans. Xyl-Ser-C12 exhibited greater acceptor activity for the glycosylation of glycosaminoglycan-type oligosaccharides than *p*-nitrophenyl-β-D-xylopyranoside.

© 2012 Elsevier Ltd. All rights reserved.

1. Introduction

Oligosaccharides, which play an important role in cellular functions, such as recognition, adhesion, and division, are attracting increasing interest in biotechnology and drug development.[1] This expanding interest has led to an increased demand for the construction of saccharide libraries to provide research materials. Several strategies involving direct extraction from natural resources, organic synthesis, and enzymatic synthesis, have been developed in order to construct oligosaccharide libraries.[2] Recently, a way to obtain oligosaccharides by administering saccharide primers to animal cells has been established. Dodecyl β-lactoside (Lac-C12),[3–5] dodecyl-acetamido-2-deoxy-β-D-glucopyranoside (GlcNAc-C12), dodecyl-β-D-galactopyranosyl-(1(4)-2-acetamido-2-deoxy-β-D-glucopyranoside (LacNAc-C12),[6] and azidododecyl β-lactoside (Lac-C12N3)[7] have been developed as saccharide primers to produce glycan libraries involving ganglio-, globo-, and neolacto-series oligosaccharides.

Glycosaminoglycans (GAGs) are known to participate in specific biological and physiological functions in cancer progression, angiogenesis, cell adhesion, and anticoagulation.[8,9] However, due to the heterogeneity and diversity of GAG structures, the relationship between their biological function and structure is not well understood.[10] Therefore, it is important to develop a method of reconstructing GAG oligosaccharides and to know the GAG biosynthetic pathway in cells for understanding their structure–function relationships.

The biosynthesis of GAGs is initiated by the formation of a tetrasaccharide linkage region composed of glucuronic acid-galactose-galactose-xylose (β-GlcA-(1→3)-β-Gal-(1→3)-β-Gal(1→4)-β-Xyl-), where Xyl is attached to a serine residue in the core protein.[10] It has been found that exogenous β-D-Xylosides such as *p*-nitrophenyl-β-D-xylopyranoside[11,12] (Xyl-pNP), methylumbelliferyl-β-D-xylopyranoside (Xyl-MU),[13] β-estradiol xylopyranoside,[14] and naphthol xyloside derivatives (XylNapOH)[15–17] could act as artificial initiators for the elongation of glycosaminoglycan chains, and primed the synthesis of glycosaminoglycan-type oligosaccharides in several types of cells. Furthermore β-D-xylosides have been found to inhibit the endogenous biosynthesis of glycosaminoglycan.[12,18]

In the present study, a novel saccharide primer, N^{α}-lauryl-*O*-(β-D-xylopyranosyl)-L-serinamide (Xyl-Ser-C12, Fig. 1), was employed as an initiator to synthesize glycosaminoglycan (GAG) oligosaccharides using the GAG biosynthesis system of cells. Xyl-Ser-C12, mimicking the region where xylose attached to the specific serine residues of the core protein, was suggested to prime the elongation of GAG chains. The glycosylation of Xyl-Ser-C12 by mammalian cells was examined.

2. Results

2.1. Chemical synthesis of Xyl-Ser-C12

The chemical synthesis of N^{α}-lauryl-*O*-(β-D-xylopyranosyl)-L-serinamide **(5)** was shown in Scheme 1. 2,3,4-Tri-*O*-acetyl-D-xylopyranosyl-trichloroacetimidate **(1)** served as the glycosyl donor. Glycosylation of **1** with *N*-α-carbobenzoxy-L-serinamide

* Corresponding author. Fax: +81 45 566 1447.
E-mail address: sato@bio.keio.ac.jp (T. Sato).

0008-6215/$ - see front matter © 2012 Elsevier Ltd. All rights reserved.
http://dx.doi.org/10.1016/j.carres.2012.08.003

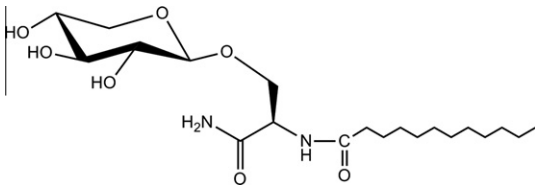

Figure 1. The structure of N^{α}-lauryl-*O*-(β-D-xylopyranosyl)-L-serinamide (Xyl-Ser-C12).

(Z-Ser-NH_2) was carried out in the presence of $BF_3{\cdot}Et_2O$. The obtained product **2** was considered to be an orthoester, and was subjected to TMSOTf-catalyzed isomerization to obtain β-anomer **3** predominantly. Conversion of **3** into **4** was carried out in a two-step synthesis involving the removal of a carbobenzyloxy group (Cbz) by catalytic hydrogenation over Pd/C and condensation with lauric acid in 41% overall yield for the two steps. Finally, N^{α}-lauryl-*O*-(β-D-xylopyranosyl)-L-serinamide **(5)** was obtained by *O*-deacetylation with methanolic NaOMe and purification by silica gel chromatography.

2.2. Glycosylation of Xyl-Ser-C12 by FBJ-S1 cells

The murine osteosarcoma cell line FBJ-S1[19,20] was employed to investigate the extent of the glycosylation of Xyl-Ser-C12. FBJ-S1 cells were incubated with 50 μM Xyl-Ser-C12 for 48 h, and the glycosylated products were isolated from the culture medium using a Sep-Pak C18 cartridge. These products were separated into neutral and acidic fractions with an aminopropyl SPE cartridge. The structures of the neutral and acidic products were analyzed by LC–MS. As shown in Table 1, two neutral products and six acidic products were detected and their structures were predicted based on MS/MS assignments (Tables 1 and 2 and Supplementary Fig. 1) and glycosidase digestion (Supplementary Fig. 3).

2.3. Analyses of the structures of the glycosylated products derived from FBJ-S1 cells

As shown in Table 1, two neutral products with *m*/*z* 615.9 $[M+Cl]^-$ (SXN1) and 777.9 $[M+Cl]^-$ (SXN2) were detected. MS/MS spectra of SXN1 revealed peaks at *m*/*z* 178.7 corresponding to the C_1 fragment ion indicating that SXN1 was Hex-Xyl-Ser-C12. The C_2 fragment ion with *m*/*z* 340.6 in the MS/MS spectra of SXN2, suggested the existence of two hexose residues in SXN2 (Table 2). The non-reducing hexose residues of SXN1 and SXN2 were cleaved by an exo-β-galactosidase (Supplementary Fig. 3A). Thus, SXN1 and SXN2 were identified as Galβ-Xyl-Ser-C12 and Galβ-Galβ-Xyl-Ser-C12, respectively. Six products with *m*/*z* 659.7 $[M-H]^-$, 870.8 $[M-H]^-$, 1032.9 $[M-H]^-$, 917.9 $[M-H]^-$, 1120.8 $[M-H]^-$, and 749.4 $[M-2H]^{2-}$ were detected in the acidic fraction (Table 1). SXA1 with *m*/*z* 659.7 was suggested to be the product having a sulfated group in Gal-Xyl-Ser-C12. The B_1 fragment with *m*/*z* 240.7 of SXA1 showed that the Gal residue was sulfated (Table 2). SXA2 was considered to be NeuAc-Gal-Xyl-Ser-C12 based on the B_1 fragment (*m*/*z* 290.2) and the B_2 fragment (*m*/*z* 451.5). SXA3 was deduced to be NeuAc-Gal-β-Gal-β-Xyl-Ser-C12 from the B_1 fragment (*m*/*z* 289.9) and the B_2 fragment (*m*/*z* 451.5). Both of the *N*-acetylneuraminic acid residues of SXA2 and SXA3 were cleaved by α-(2→3)-neuraminidase (Supplementary Fig. 3B). Thus, linkages of *N*-acetylneuraminic acid to galactose in SXA2 and SXA3 were determined to be α-(2→3). SXA4 was deduced to be GlcA-β-Gal-β-Gal-β-Xyl-Ser-C12, based on the C_2 fragment with *m*/*z* 354.8 and the digestion by β-glucuronidase (Supplementary Fig. 3C). In the MS/MS spectra of SXA5, the elongation of HexNAc and HexA to SXN2 was indicated by the Z_4 fragment with *m*/*z* 899.6 and the Y_3 fragment with *m*/*z* 742.0 (Table 2). The structure of SXA5 was considered as HexNAc-HexA-Gal-β-Gal-β-Xyl-Ser-C12. SXA6 with *m*/*z* 749.4 $[M-2H]^{2-}$ was determined to be $(HexNAc\text{-}GlcA)_2$-Gal-β-Gal-β-Xyl-Ser-C12 from the Z_6 fragment with *m*/*z* 1278.5 and the Y_5 fragment with *m*/*z* 1120.6 (Table 2).

To identify the isomer of the non-reducing HexNAc in SXA5 and SXA6 and the linkage between the HexNAc and HexA, digestion experiments using exo-type β-acetylhexosaminase and α-acetylgalactosaminidase were carried out. Since SXA5 and SXA6 were not digested by β-acetylhexosaminase, it was suggested that HexNAc was conjugated to HexA by an α-linkage (Supplementary Fig. 3D). Furthermore, since SXA5 and SXA6 were also hydrolyzed by α-acetylgalactosaminidase, HexNAc of the non-reducing end was suggested to be α-GalNAc (Supplementary Fig. 3E). The major product was SXA5 (GalNAc-α-GlcA-β-Gal-β-Gal-β-Xyl-Ser-C12).

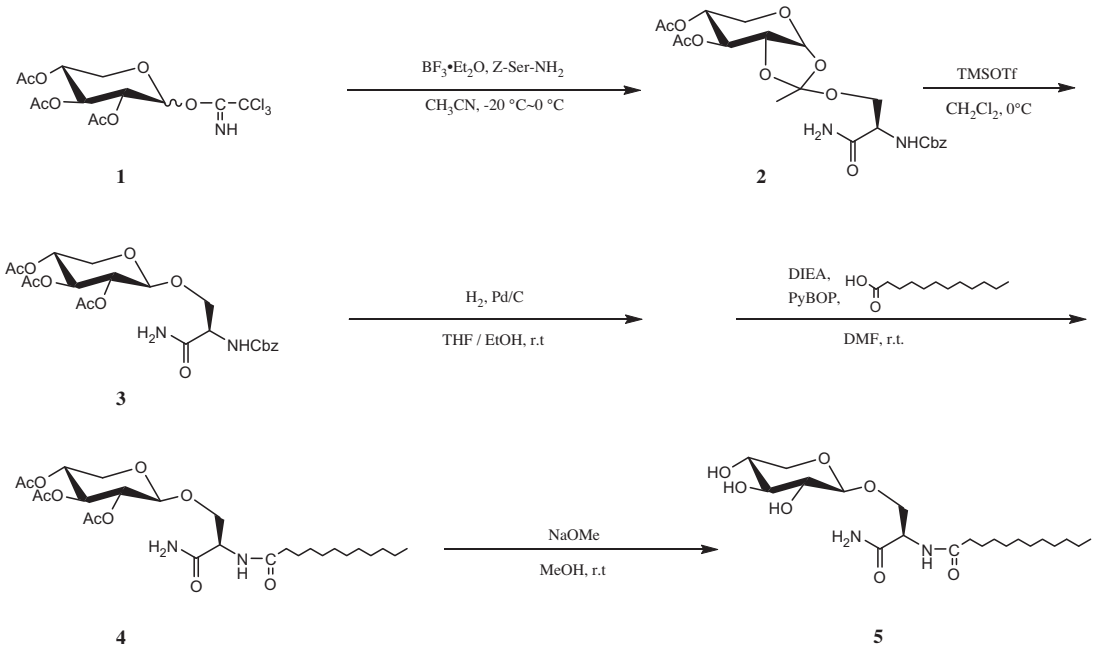

Scheme 1. Synthesis of N^{α}-lauryl-*O*-(β-D-xylopyranosyl)-L-serinamide (Xyl-Ser-C12).

Table 1
Xyl-Ser-C12 glycosylated products from FBJ cells detected by LC–MS

Product	Retention time (min)	Predicted Structures	Ion type	Observed mass (*m*/*z*)	Calculated mass (*m*/*z*)	Proportion[a] (%)
SXN1	25.3	Galβ-Xyl-Ser-C12	$[M+Cl]^-$	615.9	615.3	51.8
SXN2	32.0	Galβ-Galβ-Xyl-Ser-C12	$[M+Cl]^-$	777.9	777.3	48.2
SXA1	29.7	GalβS-Xyl-Ser-C12	$[M-H]^-$	659.7	659.3	2.6
SXA2	33.0	NeuAcα-Galβ-Xyl-Ser-C12	$[M-H]^-$	870.8	870.8	25.5
SXA3	34.1	NeuAcα-Galβ-Galβ-Xyl-Ser-C12	$[M-H]^-$	1032.9	1032.8	10.8
SXA4	34.3	GlcAβ-Galβ-Galβ-Xyl-Ser-C12	$[M-H]^-$	917.9	917.6	5.1
SXA5	37.6	GalNAcα-GlcAβ-Galβ-Galβ-Xyl-Ser-C12	$[M-H]^-$	1120.8	1120.5	52.5
SXA6	39.4	GalNAcα-(GlcAβ-GlcNAcα)-GlcAβ-Galβ-Galβ-Xyl-Ser-C12	$[M-2H]^{2-}$	749.4	749.3	3.5

[a] The proportion of each product represents the ratio of each chromatogram area to total area (Normalized by protein amount). The data for the neutral products and the acidic products were calculated separately.

Table 2
MS/MS assignment of Xyl-Ser-C12 glycosylated products from FBJ-S1 cells

Product	Fragments
SXN1	579.1 ($[M-H]^-$), 310.9 ($[C_2-H]^-$), 267.1 ($[Z_0-H]^-$), 178.7 ($[C_1-H]^-$)
SXN2	742.3 ($[M-H]^-$), 579.0 ($[Y_2-H]^-$), 472.7 ($[C_3-H]^-$), 340.6 ($[C_2-H]^-$), 322.9 ($[B_2-H]^-$)
SXA1	390.9 ($[C_2-H]^-$), 372.9 ($[B_2-H]^-$), 258.9 ($[C_1-H]^-$), 240.7 ($[B_1-H]^-$)
SXA2	601.9 ($[C_3-H]^-$), 451.4 ($[B_2-H]^-$), 290.2 ($[B_1-H]^-$), 267.3 ($[Z_0-H]^-$)
SXA3	764.2 ($[C_4-H]^-$), 742.3 ($[Y_3-H]^-$), 614.2 ($[B_3-H]^-$), 578.4($[Y_2-H]^-$), 451.5 ($[B_2-H]^-$), 289.8 ($[B_1-H]^-$)
SXA4	740.2 ($[Y_3-H]^-$), 649.4 ($[C_4-H]^-$), 517.1 ($[C_3-H]^-$), 498.8 ($[B_3-H]^-$), 354.8 ($[C_2-H]^-$), 336.8 ($[B_2-H]^-$)
SXA5	918.0 ($[Y_4-H]^-$), 899.6 ($[Z_4-H]^-$), 852.1 ($[C_5-H]^-$), 742.0 ($[Y_3-H]^-$), 720.3 ($[C_4-H]^-$) 558.9 ($[C_3-H]^-$), 395.4 ($[C_2-H]^-$)
SXA6	1278.5 ($[Z_6-H]^-$), 1231.6 ($[C_7-H]^-$), 1120.6 ($[Y_5-H]^-$), 1099.4 ($[C_6-H]^-$), 937.4 ($[C_5-H]^-$), 899.5 ($[Z_4-H]^-$) 599.1 ($[C_3-H]^-$), 395.7 ($[C_2-H]^-$)

FBJ-S1 cells were also treated with 50 μM *p*-nitrophenyl-β-D-xylopyranoside, for 2 days. Five glycosylated products were detected by LC–MS (Table 3) and their structures were deduced based on MS/MS spectra (Table 4). SPN1 with *m*/*z* 468.7 $[M+Cl]^-$ was suggested to be Hex-Xyl-pNP based on the B_1 fragment with *m*/*z* 160.8. The B_3 fragment ion with *m*/*z* 455.1 in MS/MS spectra of SPN2, suggested that the structure of SPN2 is Hex-Hex-Xyl-pNP. SPA1 with *m*/*z* 723.9 was considered to be NeuAc-Hex-Xyl-pNP based on the B_1 fragment (*m*/*z* 290.0) and the B_3 fragment (*m*/*z* 566.1). MS/MS spectra of SPA2 revealed a Z_4 fragment (*m*/*z* 752.1), Y_3 fragment (*m*/*z* 595.1), C_2 fragment (*m*/*z* 396.1), and C_3 fragment (*m*/*z* 558.1), suggesting that SPA2 was HexNAc-HexA-Hex-Hex-Xyl-pNP. For the structure of SPA3, the elongation of HexNAc-HexA to SPA2 was indicated by the Z_6 fragment (*m*/*z* 1131.3) and Z_5 fragment (*m*/*z* 956.2) in the MS/MS spectra. SPA3 was determined as $(HexNAc-HexA)_2$-Hex-Hex-Xyl-pNP.

2.4. Glycosylation of Xyl-Ser-C12 by CHO cells

The glycosylation of Xyl-Ser-C12 was also examined using CHO cells. Two neutral products and 14 acidic products were detected, and their structures were determined as shown in Table 5. MS/MS assignments are shown in Table 6. CXN1 (*m*/*z* 615.9 $[M+Cl]^-$) was deduced to be Gal-β-Xyl-Ser-C12 from the C_1 fragment with *m*/*z* 178.7 and β-galactosidase digestion (Supplementary Fig. 6A). CXN2 was deduced to be Gal-β-Gal-β-Xyl-Ser-C12 from MS/MS spectra (B2 and Y2 fragments) and β-galactosidase digestion (Supplementary Fig. 6A).

Among the acidic products, CXA1 with *m*/*z* 659.7 was considered to be the structure elongating the sulfated Gal residue to Xyl-Ser-C12 from the B_1 fragment with *m*/*z* 240.7. CXA2 was deduced to be NeuAc-Gal-Xyl-Ser-C12. The B_1 fragment (*m*/*z* 289.6) and the B_2 fragment (*m*/*z* 451.9) suggested the presence of NeuAc-Gal in CXA2. CXA3 was deduced to be NeuAc-Gal-β-Gal-β-Xyl-Ser-C12, based on the B_1 fragment (*m*/*z* 290.0) and the B_3 fragment (*m*/*z* 614.0). The linkage of NeuAc-Gal in CXA2 and CXA3 was determined as α-(2→3) with hydrolysis using α2-3 neuraminidase (Supplementary Fig. 6B). CXA4 was deduced to be HexA-Gal-Gal-Xyl-Ser-C12 based on the C_2 fragment with *m*/*z* 355.0. The HexA residue was determined as GlcA by the hydrolysis with β-glucuronidase (Supplementary Fig. 6C). The structure of CXA5 was identified as HexNAc-HexA-Gal-Gal-Xyl-Ser-C12 from the Z_4 fragment (*m*/*z* 899.5) and Y_3 fragment (*m*/*z* 742.2). A sulfated product, CXA6, was also detected, and the sulfated position was determined as Gal linked to Xyl from the Y_4 fragment (*m*/*z* 997.3), Z_4 fragment (*m*/*z* 979.2), Y_3 fragment (*m*/*z* 820.9), and Y_2 fragment (*m*/*z* 659.8). CXA7 with *m*/*z* 648.3 was deduced to be GlcA-HexNAc-GlcA-Gal-Gal-Xyl-Ser-C12 from the Z_5 fragment (*m*/*z* 1120.2) and C_1 fragment (*m*/*z* 192.8).

Table 3
Xyl-pNP glycosylated products from FBJ-S1 cells detected by LC–MS

Product	Retention time (min)	Predicted structures	Ion type	Observed mass (*m*/*z*)	Calculated mass (*m*/*z*)	Proportion[a] (%)
SPN1	20.6	Hex-Xyl-pNP	$[M+Cl]^-$	468.7	468.1	18.5
SPN2	29.1	Hex-Hex-Xyl-pNP	$[M+Cl]^-$	630.8	630.1	81.5
SPA1	33.1	NeuAc-Hex-Xyl-pNP	$[M-H]^-$	723.9	723.2	6.1
SPA2	35.1	HexNAc-HexA-Hex-Hex-Xyl-pNP	$[M-H]^-$	974.0	973.3	92.5
SPA3	41.2	HexNAc-HexA-HexNAc-HexA-Hex-Hex-Xyl-pNP	$[M-2H]^{2-}$	676.9	676.7	1.5

[a] The proportion of each product represents the ratio of each chromatogram area to total area (Normalized by protein amount). The data for the neutral products and the acidic products were calculated separately.

Table 4
MS/MS assignment of Xyl-pNP glycosylated products from FBJ-S1 cells

Product	Fragments
SPN1	432.8 ($[M-H]^-$), 160.8 ($[B_1-H]^-$)
SPN2	594.7 ($[M-H]^-$), 455.1 ($[B_3-H]^-$)
SPA1	583.9 ($[C_3-H]^-$), 566.1 ($[B_3-H]^-$), 290.0 ($[B_1-H]^-$)
SPA2	835.3 ($[C_5-H]^-$), 752.1 ($[Z_4-H]^-$), 720.2 ($[C_4-H]^-$), 595.1 ($[Y_3-H]^-$), 558.1 ($[C_3-H]^-$), 396.1 ($[C_2-H]^-$)
SPA3	1213.6 ($[B_7-H]^-$), 1131.3 ($[Z_6-H]^-$), 1099.2 ($[C_6-H]^-$), 956.2 ($[Z_5-H]^-$), 937.2 ($[C_5-H]^-$), 752.2 ($[Z_4-H]^-$), 598.7 ($[C_3-H]^-$)

Table 5
Xyl-Ser-C12 glycosylated products from CHO cells detected by LC–MS

Product	Retention time (min)	Predicted structures	Ion type	Observed mass (*m*/*z*)	Calculated mass (*m*/*z*)	Proportion[a] (%)
CXN1	25.1	Galβ-Xyl-Ser-C12	$[M+Cl]^-$	615.9	615.3	59.7
CXN2	30.4	Galβ-Galβ-Xyl-Ser-C12	$[M+Cl]^-$	777.9	777.3	40.3
CXA1	30.6	GalβS-Xyl-Ser-C12	$[M-H]^-$	659.7	659.3	3.3
CXA2	31.6	NeuAcα-Galβ-Xyl-Ser-C12	$[M-H]^-$	870.9	870.4	14.0
CXA3	32.8	NeuAcα-Galβ-Galβ-Xyl-Ser-C12	$[M-H]^-$	1032.9	1032.5	14.8
CXA4	33.1	GlcAβ-Galβ-Galβ-Xyl-Ser-C12	$[M-H]^-$	917.8	917.4	23.6
CXA5	33.9	GalNAcα-GlcAβ-Galβ-Galβ-Xyl-Ser-C12	$[M-H]^-$	1121.0	1120.5	24.6
CXA6	34.7	GalNAcα-GlcAβ-Galβ-GalβS-Xyl-Ser-C12	$[M-2H]^{2-}$	600.3	599.7	3.7
CXA7	35.3	GlcA-GlcNAcα-GlcAβ-Galβ-Galβ-Xyl-Ser-C12	$[M-2H]^{2-}$	648.3	647.8	3.8
CXA8	39.1	GalNAcα-(GlcA-GlcNAcα)-GlcAβ-Galβ-Galβ-Xyl-Ser-C12	$[M-2H]^{2-}$	749.9	749.3	9.7
CXA9	41.1	GalNAcαS-(GlcA-GalNAcα)-GlcAβ-Galβ-Galβ-Xyl-Ser-C12	$[M-2H]^{2-}$	789.9	789.3	0.1
CXA10	44.9	(GlcA-GalNAcα) 2-GlcAβ-Galβ-Galβ-Xyl-Ser-C12 [	$[M-2H]^{2-}$	837.9	837.3	0.4
CXA11	46.2	GalNAcα-$(GlcA-GalNAcα)_2$-GlcAβ-Galβ-Galβ-Xyl-Ser-C12	$[M-2H]^{2-}$	939.2	938.8	1.3
CXA12	47.1	GalNAcαS-$(GlcA-GalNAcα)_2$-GlcAβ-Galβ-Galβ-Xyl-Ser-C12	$[M-2H]^{2-}$	979.2	978.9	0.1
CXA13	49.7	(GlcA-GalNAcα) 3-GlcAβ-Galβ-Galβ-Xyl-Ser-C12	$[M-2H]^{2-}$	1027.3	1026.9	0.2
CXA14	50.7	GalNAcα-$(GlcA-GalNAcα)_3$-GlcAβ-Galβ-Galβ-Xyl-Ser-C12	$[M-2H]^{2-}$	1128.9	1128.4	0.5

[a] The proportion of each product represents the ratio of each chromatogram area to total area (Normalized by protein amount). The data for the neutral products and the acidic products were calculated separately.

Table 6
MS/MS assignment of Xyl-Ser-C12 glycosylated products from CHO cells

Product	Fragments
CXN1	579.2 ($[M-H]^-$), 310.8 ($[C_2-H]^-$), 267.0 ($[Z_0-H]^-$), 178.7 ($[C_1-H]^-$)
CXN2	742.3 ($[M-H]^-$), 579.2($[Y_2-H]^-$), 473.2 ($[C_3-H]^-$), 341.3 ($[C_2-H]^-$), 322.9 ($[B_2-H]^-$)
CXA1	390.9 ($[C_2-H]^-$), 373.4 ($[B_2-H]^-$), 259.3 ($[C_1-H]^-$), 240.7 ($[B_1-H]^-$)
CXA2	602.1 ($[C_3-H]^-$), 451.9 ($[B_2-H]^-$), 289.6 ($[B_1-H]^-$), 267.2($[Z_0-H]^-$)
CXA3	764.0 ($[C_4-H]^-$), 742.2($[Y_3-H]^-$), 614.0 ($[B_3-H]^-$), 578.2 ($[Y_2-H]^-$), 290.0 ($[B_1-H]^-$)
CXA4	739.7 ($[Y_3-H]^-$), 649.1 ($[C_4-H]^-$), 516.9 ($[C_3-H]^-$), 498.8 ($[B_3-H]^-$), 355.0 ($[C_2-H]^-$), 336.7 ($[B_2-H]^-$)
CXA5	918.1 ($[Y_4-H]^-$), 899.4 ($[Z_4-H]^-$), 852.0 ($[C_5-H]^-$), 742.2 ($[Y_3-H]^-$), 720.4 ($[C_4-H]^-$), 559.1 ($[C_3-H]^-$)
CXA6	1120.6 ($[Y_5-H]^-$), 1099.4 ($[C_6-H]^-$), 997.3 ($[Y_4-H]^-$), 979.2 ($[Z_4-H]^-$]), 932.2 ($[C_5-H]^-$), 899.8 ($[Z_4-H]^-$), 820.9 ($[Y_3-H]^-$), 659.8 ($[Y_2-H]^-$), 620.0 ($[B_3-H]^-$), 539.5 ($[B_3-H]^-$), 458.0 ($[B_2-H]^-$), 378.0 ($[B_2-H]^-$)
CXA7	1120.2 ($[Y_5-H]^-$), 1028.3 ($[C_6-H]^-$), 899.5 ($[Z_4-H]^-$), 880.3 ($[B_5-H]^-$), 734.2 ($[C_4-H]^-$) 554.0 ($[B_3-H]^-$), 396.0 ($[C_2-H]^-$), 192.8 ($[C_1-H]^-$)
CXA8	1278.6 ($[Z_6-H]^-$), 1231.2 ($C_7-H]^-$), 1120.6 ($[Y_5-H]^-$), 1100.2 ($[C_6-H]^-$), 937.4 ($[C_5-H]^-$), 899.4 ($[Z_4-H]^-$), 775.7 ($[C_4-H]^-$), 740.7 ($[Y_3-H]^-$), 599.2 ($[C_3-H]^-$), 396.1 ($[C_2-H]^-$)
CXA9	1296.4 ($[Y_6-H]^-$), 1120.3 ($[Y_5-H]^-$), 917.2 ($[Y_4-H]^-$), 899.5 ($[Z_4-H]^-$), 775.6 ($[C_4-H]^-$) 661.2 ($[B_3-H]^-$), 458.0 ($[B_2-H]^-$), 299.6 ($[C_1-H]^-$), 281.9 ($[B_1-H]^-$)
CXA10	1500.4 ($[Y_7-H]^-$), 1407.3 ($[C_8-H]^-$), 1296.5 ($[Y_6-H]^-$), 1120.3 ($[Y_5-H]^-$), 1113.4 ($[C_6-H]^-$), 933.2 ($[B_5-H]^-$), 899.2 ($[Z_4-H]^-$), 775.3 ($[C_4-H]^-$), 741.6 ($[Y_3-H]^-$), 572.0 ($[C_3-H]^-$), 396.2 ($[C_2-H]^-$)
CXA11	1658.6 ($[Z_8-H]^-$), 1499.7 ($[Y_7-H]^-$), 1316.7 ($[C_7-H]^-$), 1296.5 ($[Y_6-H]^-$), 1136.2 ($[B_6-H]^-$), 1120.5 ($[Y_5-H]^-$), 978.3 ($[C_5-H]^-$), 917.5 ($[Y_4-H]^-$), 775.1 ($[C_4-H]^-$), 741.6 ($[Y_3-H]^-$), 599.3 ($[C_3-H]^-$), 396.2 ($[C_2-H]^-$)
CXA12	1658.6 ($[Z_8-H]^-$), 1499.6 ($[Y_7-H]^-$), 1378.6 ($[B_7-H]^-$), 1296.5 ($[Y_6-H]^-$), 1234.6 ($[C_6-H]^-$), 1120.3 ($[Y_5-H]^-$), 1040.2 ($[B_5-H]^-$), 917.3 ($[Y_4-H]^-$), 869.1 ($[Z_8-2H]^{2-}$), 837.2 ($[B_4-H]^-$), 789.2 ($[Y_7-2H]^{2-}$), 458.1 ($[B_2-H]^-$)
CXA13	1879.5 ($[Y_9-H]^-$), 1675.5 ($[Y_8-H]^-$), 1499.7 ($[Y_7-H]^-$), 1312.4 ($[C_7-H]^-$), 1296.5 ($[Y_6-H]^-$), 1154.2 ($[C_6-H]^-$), 1120.5 ($[Y_5-H]^-$), 950.9 ($[C_5-H]^-$), 917.2 ($[Y_4-H]^-$), 776.1 ($[C_4-H]^-$), 571.7 ($[C_3-H]^-$), 396.0 ($[C_2-H]^-$)
CXA14	1878.9 ($[Y_9-H]^-$), 1675.7 ($[Y_8-H]^-$), 1515.3 ($[B_8-H]^-$), 1499.7 ($[Y_7-H]^-$), 1339.3 ($[B_7-H]^-$), 1296.5 ($[Y_6-H]^-$), 1136.2 ($[B_6-H]^-$), 1120.4 ($[Y_5-H]^-$), 960.4 ($[B_5-H]^-$), 917.3 ($[Y_4-H]^-$), 757.2 ($[B_4-H]^-$), 581.3 ($[B_3-H]^-$), 396.1 ($[C_2-H]^-$)

CXA8 with *m*/*z* 749.9 was deduced to be $(HexNAc-GlcA)_2$-Gal-Gal-Xyl-Ser-C12 from MS/MS spectra with the Z_6 fragment (*m*/*z* 1278.6) and Y_5 fragment (*m*/*z* 1120.2). Longer glycosylated products, such as CXA11-14 and $(HexNAc-GlcA)_n$-Gal-Gal-Xyl-Ser-C12, were detected for CHO cells. Sulfated products such as CXA9 and CXA12 were also detected. The terminal HexNAc of CXA9 was considered to be sulfated based on the Y_6 fragment (*m*/*z* 1296.4) and B_1 fragment (*m*/*z* 281.9). The terminal HexNAc of CXA12 was deduced to be sulfated from the Z_8 fragment with *m*/*z* 1658.6 and the dominant presence of the Y_7 fragment with *m*/*z* 1499.6.

Table 7
Xyl-pNP glycosylated products from CHO cells detected by LC–MS

Product	Retention time (min)	Predicted structures	Ion type	Observed mass (*m*/*z*)	Calculated mass (*m*/*z*)	Proportion[a] (%)
CPN1	19.0	Hex-Xyl-pNP	$[M+Cl]^-$	468.8	468.1	12.4
CPN2	28.5	Hex-Hex-Xyl-pNP	$[M+Cl]^-$	630.9	630.1	87.6
CPA1	32.6	NeuAc-Hex-Xyl-pNP	$[M-H]^-$	723.4	723.2	8.5
CPA2	35.4	HexNAc-HexA-Hex-Hex-Xyl-pNP	$[M-H]^-$	973.6	973.3	90.8
CPA3	42.5	HexNAc-HexA-HexNAc-HexA-Hex-Hex-Xyl-pNP	$[M-2H]^{2-}$	676.5	676.7	0.7

[a] The proportion of each product represents the ratio of each chromatogram area to total area (Normalized by protein amount). The data for the neutral products and the acidic products were calculated separately.

Table 8
MS/MS assignment of Xyl-pNP glycosylated products from CHO cells

Product	Fragments
CPN1	432.7 ($[M-H]^-$), 178.8 ($[C_1-H]^-$)
CPN2	594.0 ($[M-H]^-$), 455.0 ($[B_3-H]^-$)
CPA1	583.9 ($[C_3-H]^-$), 470.1 ($[C_2-H]^-$), 289.9 ($[B_1-H]^-$)
CPA2	834.1 ($[C_5-H]^-$), 752.1 ($[Z_4-H]^-$), 719.9 ($[C_4-H]^-$), 595.0 ($[Y_3-H]^-$), 558.1 ($[C_3-H]^-$), 396.0 ($[C_2-H]^-$)
CPA3	1213.4 ($[B_7-H]^-$), 1131.1 ($[Z_6-H]^-$), 1099.4 ($[C_6-H]^-$), 956.2 ($[Z_5-H]^-$), 937.2 ($[C_5-H]^-$), 752.2 ($[C_4-H]^-$) 598.7 ($[Z_3-H]^-$), 396.9 ($[C_2-H]^-$)

HexNAc residues of the non-reducing end in products such as CXA5 derived from CHO cells were determined to be α-GalNAc by hydrolysis with α-acetylgalactosaminidase (Supplementary Fig. 6E). Since products with several repeating units of HexNAc-GlcA, such as CXA8, were cleaved by heparitinase, it was indicated that Xyl-Ser-C12 was glycosylated by the biosynthesis of heparan sulfate (Supplementary Fig. 6F). The major products were CXA4 (GlcA-β-Gal-β-Gal-β-Xyl-Ser-C12, 23.6%) and CXA5 (GalNAc-α-GlcA-β-Gal-β-Gal-β-Xyl-Ser-C12, 24.6%).

The glycosylation reaction in CHO cells was also examined using Xyl-pNP. Under reaction conditions similar to those for Xyl-Ser-C12, five products were detected (Table 7). Their structures were predicted based on MS/MS assignments (Table 8) and the exploration of structures of Xyl-pNP-initiated products by Salimath et al.[21] Only short products were detected for Xyl-pNP compared to Xyl-Ser-C12. The major product was CPA2, GalNAc-GlcA-Gal-Gal-Xyl-pNP (92.5% of acidic products). A sialyted product (CPA1) was also detected.

2.5. The viability of cells treated with Xyl-Ser-C12

FBJ-S1 or CHO cells were treated with 50 μM Xyl-Ser-C12, 50 μM Xyl-pNP, or an equal volume of DMSO in culture medium for 2 days. Cytotoxicity was investigated by cell morphology and WST assays. Compared with the control without saccharide primers, no obvious toxic effects were observed (Supplementary Fig. 7).

3. Discussion

A series of β-D-xylosides including *p*-nitrophenyl-β-D-xylopyranoside[11] (Xyl-pNP), methylumbelliferyl-β-D-xylopyranoside,[13] β-estradiol xylopyranoside,[14] and naphthol xyloside derivatives (XylNapOH)[15–17] have been developed as initiators of GAGs or inhibitors of endogenous GAGs. Most of these xylosides primed the production of short oligosarccharides, mainly consisting of xylosides with Gal-Xyl-R, Gal-Gal-Xyl-R, and NeuAc-Gal-Gal-Xyl-R. High molecular weight GAG chains usually comprise minor xyloside products.[22] Thus, we attempted to develop a novel saccharide primer (Xyl-Ser-C12) for synthesizing GAG-type oligosaccharides. The saccharide primer synthesized in the present study contained xylose, serine, and dodecanoyl groups. Such a chemical structure was expected to function as a good artificial substrate for glycosyltransferases to obtain GAG-type oligosaccharides.

In the present study, Xyl-Ser-C12 and Xyl-pNP were added to cells, and the glycosylated products were isolated and analyzed. The Xyl-Ser-C12 primer produced more and longer species of glycosylated products, than did Xyl-pNP, especially in CHO cells. We hypothesized that the hydrophobicity of the aglycones may influence the uptake of the β-Xylosides by cells, the localization in subcellular compartments, and the secretion of the glycosylated products,[23,24] consequently affecting the composition of the glycosylated products, though the current study focused on the synthesis of Xyl-Ser-C12 and the structures of the glycosylated products.

Longer products (CXA11-14) having several repeating units of disaccharides and more sulfated products (CXA9, 12) were detected with Xyl-Ser-C12 than Xyl-pNP. The profile of Xyl-pNP-primed oligosaccharides follows a similar pattern to that reported in the literature.[21] When FBJ-S1 cells were treated with Xyl-Ser-C12, eight glycosylated products were detected. In contrast, only five products were detected after treatment with Xyl-pNP. Sulfated Gal-Xyl-R (SXA1) was detected in products from Xyl-Ser-C12 but not in products from Xyl-pNP. These results suggested that Xyl-Ser-C12 exhibited better acceptor activity for the glycosylation of xyloside to obtain GAG-type oligosaccharide or intermediates of GAG chains. The differences in the variety of glycosylated products between CHO and FBJ-S1 cells may partially reflect the profile of biosynthesis in these cells and the activity of glycoside transferases.

It has been reported that the sialyted structure α-NeuAc-(2→3)-Gal-Xyl-R, which is unrelated to the biosynthesis pathway of GAG, was produced when various cells were fed with β-xylosides, such as Xyl-pNP and Xyl-MU.[21,25–27] Etchison et al. demonstrated that α-(2→3)-sialyltransferase was co-localized with GAG core-specific galactosyltransferase I at the same Golgi apparatus.[10,28] Therefore NeuAc-Gal-Xyl was synthesized in cells by the recognition of α-(2→3)-sialyltransferase. However, another sialyted product (SXA3 or CXA3), α-NeuAc-(2→3)-Gal-Gal-Xyl-R, has not been reported. Detection of these products may suggest the co-localization of GAG core-specific glucuronic acid transferase I and α-(2→3)-sialyltransferase.[10,28]

α-GalNAc-capped xylosides, such as SXA5, SXA6, CXA5, and CXA8, were also detected in the glycosylated products. Miura et al. have previously reported that α-GalNAc-capped structures were produced by several cell lines when incubated with 4-methylumbelliferyl (MU) or *p*-nitrophenyl (pNP) β-D-xylosides.[21,25] Kitagawa et al. have clarified that glycosyltransferase EXTL2, which transfers α-GlcNAc to GlcA of the GAG linker region in the biosynthesis of

heparan sulfate, also transferred α-GalNAc.[29,30] Though the significance of the α-GalNAc-cap's modification is still unknown it seems that the addition of α-GalNAc resulted in termination of the extension of the GAG chain.

Artificial β-D-Xylosides such as Xyl-pNP and Xyl-MU preferentially primed the elongation of chondroitin sulfate (CS) and only weakly initiated the synthesis of heparan sulfate chains (HS).[11,27] It has been reported that the aglycone structure of these xylosides could affect the proportion of CS or HS made on these β-D-xylosides. Xylosides with hydrophobic aglycone structures, such as estradiol β-D-xyloside and naphthol β-D-xyloside, could initiate the synthesis of HS effectively in various types of cells.[14,17,24] However, a clear correlation between the aglycone structure and the composition of products (proportion of CS/HS) has not been found. In the present study, products such as SXA6 and CXA8 were hydrolyzed by heparitinase, suggesting that Xyl-Ser-C12 could stimulate the elongation of HS GAGs. On the other hand, products such as SXA2 and CXA2, in which galactose residues were sulfated, were detected. It has been reported that sulfation on the galactose of the linker region occurred in the biosynthesis of CS, but not HS.[10,31,32] The endogenous expression profiles of CS and HS have been extensively reported.[33] It also could be inferred that the biosynthesis of both CS and HS co-exist in mouse osteosarcoma cells based on Basappa et al.'s study[34] and the detection of the expression of GAG/proteoglycans and GAG-related glycosyltransferases in mouse osteosarcoma cells (unpublished data by Wang et al.). Thus, it is reasonable to assume that the products obtained from Xyl-Ser-C12 were synthesized by the two pathways for HS and CS.

Because glycans play important roles in living systems, there is an urgent need to develop high-throughput and large-scale glycomics for analysis of the structure and functions of sugar chains. The glycan microarray using synthetic or natural oligosaccharide libraries immobilized on solid surfaces is a useful tool for glycomics research. The saccharide primer method is an efficient complementary method for oligosaccharide synthesis. Introduction of an azido group into the alkyl chain of saccharide primers could be used in immobilization on sensor chips, and facilitate the achievement of an efficient high-throughput glycan array.[23,35] Xyl-Ser-C12-initiated oligosaccharides are also expected to be applied in glycan arrays after chemical modification.

In summary, Xyl-Ser-C12 was synthesized to obtain GAG-type oligosaccharides using mammalian cells and exhibited good ability to prime the elongation of oligosaccharides. The glycosylated products were detected by LC–MS, and the sequences of the products were determined by enzymatic digestion and MS/MS. This study should contribute to the comparison of glycosaminoglycan expression between different cell lines and the construction of glycosaminoglycan saccharide libraries.

4. Experimental

4.1. Synthesis of N^{α}-lauryl-*O*-(β-D-xylopyranosyl)-L-serinamide (Xyl-Ser-C12)

4.1.1. N^{α}-Benzyloxycarbonyl-*O*-(2,3,4-tri-*O*-acetyl-β-D-xylopyranosyl)-L-serinamide (3)

Xylose was acetylated with acetic anhydride and sodium acetate.[36] Selective 1-*O*-deacetylation of acetylated xyloside[37,38] was carried out, and the glycosyl donor, 2,3,4-tri-*O*-acetyl-D-xylopyranosyl-tricholoroacetimidate (**1**), was synthesized by Schmidt activation.[39,40] The glycosyl donor **1** was identified from NMR spectroscopy.[39]

0.100 g of **1**[39,40] (0.238 mmol, 1.0 equiv) and 0.068 g of Z-Ser-NH_2 (*N*-α-Carbobenzoxy-L-serinamide, 0.285 mmol, Watanabe Chemical Industries) were added into a 2-neck flask. The flask was evacuated, dried, and refilled with argon. After 7.0 mL of anhydrous acetonitrile was added, the reaction system was chilled to −20 °C. Then 2.9 μL of $BF_3{\cdot}Et_2O$ (0.023 μmol) was added drop wise to trigger the reaction. The resulting mixture was stirred at −20 °C overnight. The reaction was stopped by adding a drop of triethylamine. After celite filtration, the reaction solution was washed with saturated aqueous $NaHCO_3$ three times and dried over Na_2SO_4 overnight. The mixture was filtered through a cotton plug. After removal of the solvent by vacuum distillation, purification of the crude product by silica column chromatography (2.5 cm Φ × 15 cm, hexane/ethyl acetate = 2/5) afforded **2**. The compound was considered to be an orthoester formed during glycosylation, and was subjected to TMSOTf-catalyzed isomerization. TMSOTf (22 μL, 0.120 μmol, 0.4 equiv) was added to a solution of 0.740 g of **2** (0.081 mmol, 1.0 equiv) in 2 mL of anhydrous dichloromethane in an ice bath with argon protection. The next day, the reaction mixture was washed with saturated aqueous $NaHCO_3$, dried over $MgSO_4$, and subjected to reduced pressure to remove the solvent and to purification by silica column chromatography (2.5 cm Φ × 15.0 cm, hexane/ethyl acetate = 1/3) to yield compound **3** (0.013 g, 31.5%). ^{1}H NMR($CDCl_3$): δ 7.36 (m, 5H, Cbz·C_6H_5), 6.30 (s, 1H, NH_2), 5.68–5.70 (d, $J_{CH,NH}$ 6.2 Hz, 1H, Ser·NH), 5.47 (s, 1H, NH_2), 5.16–5.19 (dd, $J_{2,3}$ 8.3 Hz, $J_{3,4}$ 8.9 Hz, 1H, H-3), 5.12 (m, 2H, Cbz·CH_2), 4.94–4.96 (ddd, $J_{3,4}$ 8.9 Hz, $J_{4,5a}$ 6.2 Hz, $J_{4,5e}$ 10.3 Hz, 1H, H-4), 4.90–4.93 (dd, $J_{1,2}$ 6.2 Hz, $J_{2,3}$ 8.2 Hz, 1H, H-2), 4.53–4.54 (d, $J_{1,2}$ 6.2 Hz, 1H, H-1), 4.41 (m, $J_{6a,7}$ 3.4 Hz, 1H, H-7), 4.17–4.20 (dd, $J_{6a,7}$ 3.4 Hz, J_{gem} 10.3 Hz, 1H, H-6a), 4.11–4.14 ($J_{4,5a}$ 6.2 Hz, J_{gem} 10.3 Hz, 1H, H-5a), 3.66–3.69 (dd, J_{gem} 10.3 Hz, 1H, H-6b), 3.36–3.40 (dd, $J_{4,5e}$ 10.3 Hz, J_{gem} 10.3 Hz, 1H, H-5e), 2.03–2.05 (s, 9H, -OAc).

4.1.2. N^{α}-Lauryl-*O*-(2,3,4-tri-*O*-acetyl-β-D-xylopyranosyl)-L-serinamide (4)

To a solution of 0.050 g of compound **3** (0.100 mmol) dissolved in 10 mL of THF and 5.0 mL of EtOH, was added slowly 0.200 g of Pd/C (Aldrich) with stirring. This mixed solution was subjected to de-protection by hydrogen bubbling for 20 min (H_2 was generated by a hydrogen generator, GL Sciences). When TLC indicated the completion of the reaction, the reaction was terminated by stopping hydrogen generation. Then 28.0 μL of 4 M hydrogen chloride in 1,4-dioxane (Kokusan Chemical) was added to the mixture. Then after the removal of Pd/C through celite filtration, the filtrate was evaporated and condensed to obtain a white crystal. Without further purification, the product was subjected to the next reaction: 0.072 g of the compound obtained above and 0.050 mg of lauric acid (0.250 mmol) were added in a 2-neck flask and dissolved in 5.0 mL of anhydrous DMF under argon protection. To this solution, 44 μL of triethylamine (0.320 μmol) was added. Then 0.038 g of EDC (1-ethyl-3-(3-dimethyl-aminopropyl) carbodiimide, 0.198 mmol, Dojindo), and 0.055 g of HOBt (1-hydroxybenzotriazole, 0.407 mmol, Nova Biochem) were added to start the reaction in an ice bath. After confirmation of the disappearance of the reactant by TLC, the reaction mixture was evaporated to remove DMF. The residue was dissolved in chloroform, washed with water, and dried over Na_2SO_4, followed by removal of the solvent by vacuum distillation. The crude product was purified by silica column chromatography (2.5 cm Φ × 15.0 cm, hexane/ethyl acetate = 1/20) to obtain **4**. Yield: 41.1% (0.035 g). ^{1}H NMR ($CDCl_3$): δ 6.32–6.34 (d, $J_{CH,NH}$ 6.8 Hz, 2H, NH_2, N*H*), 5.35 (s, 1H, NH_2), 5.01–5.17 (dd, $J_{2,3}$ 8.9 Hz, $J_{3,4}$ 9.2 Hz, 1H, H-3), 4.87–4.93 (ddd, $J_{3,4}$ 9.2 Hz, $J_{4,5}$ 9.0 Hz, $J_{4,5b}$ 5.5 Hz, 1H, H-4), 4.84–4.85 (dd, $J_{1,2}$ 7.0 Hz, $J_{2,3}$ 8.9 Hz, 1H, H-2), 4.53–4.61 (m, 1H, H-7), 4.51–4.53 (d, $J_{1,2}$ 7.2 Hz, 1H, H-1), 4.08–4.12 (dd, $J_{4,5b}$ 5.9 Hz, J_{gem} 11.6 Hz, 1H, H-5e), 4.03–4.08 (dd, J_{gem} 11.0 Hz, 1H, H-6a), 3.53–3.59 (dd, J_{gem} 10.3 Hz, 1H, H-6b), 3.31–3.38 (dd, $J_{4,5a}$ 9.4 Hz, J_{gem} 11.7 Hz, 1H, H-5a), 2.14–2.19 (t, 2H, COCH_2), 1.93–2.00 (m, 9H, acetyl

group), 1.47–1.62 (m, 2H, $COCH_2CH_2$), 1.15–1.30 (m, 16H, $(CH_2)_8CH_3$), 0.78–0.88 (t, 3H, $COCH_2CH_2$ $(CH_2)_8CH_3$).

4.1.3. N^{α}-lauryl-*O*-(β-D-xylopyranosyl)-L-serinamide (5)

0.530 g of compound **4** (0.973 mmol) was mixed with 10.0 mL of methanol. To this mixture was added 10 drops of sodium methoxide methanol solution. After 45 min when TLC indicated disappearance of the reactants, activated amberlite was added to neutralize the reaction system. Then the reaction mixture was filtered through a cotton plug to remove amberlite, and vacuum distilled to remove the solvent. The product was purified by chromatography on a silica column (3.0 cm $\Phi \times 25.0$ cm, chloroform/methanol = 6/1), yielding **5** (0.249 g, 61.1%). The characteristics of **5** are as follows: Melting point: 151.9 °C (Barnstead International, Melting-point apparatus 1201D); Optical rotation: $[\alpha]_D^{24.7}$ 41.2 (JASCO, Polarimeter P-1020) (cell length: 100 mm, 24.7 °C, $c = 1.0$ g/mL, $\lambda = 589$ nm). ^{1}H NMR (CD_3OD): δ 4.46–4.49 (dd, $J_{CH,CH2}$ 4.8 Hz, 1H, H-7), 4.11–4.14 (d, $J_{1,2}$ 7.3 Hz, 1H, H-1), 4.02–4.07 (dd, $J_{CH,CH2}$ 4.8 Hz, J_{gem} 5.3 Hz, 1H, H-6b), 3.73–3.79 (dd, $J_{5a,5b}$ 11.4 Hz, 1H, H-5b), 3.59–3.63 (dd, $J_{CH,CH2}$ 4.8 Hz, J_{gem} 5.3 Hz, 1H, H-6a), 3.33–3.44 (m, 2H, H-3, H-4), 3.06–3.13 (m, $J_{1,2}$ 7.3 Hz, $J_{5a,5b}$ 11.4 Hz, 2H, H-2, H-5a), 2.16–2.21 (dd, 2H, $COCH_2$), 1.52 (m, 2H, $COCH_2CH_2$), 1.20 (m, 16H, $(CH_2)_8CH_3$), 0.78–0.82 (t, 3H, CH_3). ^{13}C NMR (CD_3OD): δ 105.35 (C-1), 77.75 (C-3), 77.74 (C-2), 71.16 (C-4), 70.61 (Ser CH_2), 67.06 (C-5), 54.37 (Ser CH), 36.93 ($COCH_2$), 33.12, 30.79, 30.69, 30.55, 30.52, 30.41, 23.77 ($(CH_2)_8CH_3$), 26.81 ($COCH_2CH_2$), 14.48 (CH_3). HRESIMS Cald. for $C_{20}H_{38}N_2O_7$: $[M+Na]^+$, 441.2571. Found: $[M+Na]^+$, 441.2565.

4.2. Cell lines and culture

The mouse osteosarcoma cell line FBJ-S1 was produced from a FBJ virus-induced osteosarcoma of the BALB/c mouse.[20,41] The cells were maintained in RPMI-1640 medium (Nacalai, Japan) supplemented with 10% FBS (GIBCO, USA) as described previously.[42] CHO (Chinese hamster ovary) cells were cultured in Ham's F-12 medium (Nacalai, Japan) supplemented with 10% heat-inactivated fetal bovine serum, 0.1 g/L streptomycin, and 50,000 units/L penicillin G potassium at 37 °C in a humidified atmosphere containing 5% CO_2.

4.3. Administration of saccharide primers

FBJ-S1 cells (2×10^6) or CHO cells (2×10^6) seeded into 100-mm culture dishes were incubated with serum-free and phenol red-free RPMI-1640 medium (Gibco) containing 50 μM Xyl-Ser-C12 or Xyl-pNP (Seikagaku), 5 mg/L of transferrin, 5 mg/L of insulin, and 30 nM selene dioxide for 48 h. The glycosylated products were collected from the culture medium using a Sep-Pak C18 cartridge (Waters, Ireland). The products were eluted with methanol. For the analysis by LC–MS, the glycosylated products were dissolved in 1 ml of chloroform/methanol (C/M) (19/1, v/v) and adsorbed to a discovery DSC–NH_2 cartridge (SUPELCO, USA). After washing of the cartridge with chloroform, the acidic products were eluted with 3% acetic acid/4% triethylamine in methanol. The eluates were passed through a minisart RC4 filter (pore size; 0.2 μm) (Satorius Stedim Biotech, Germany), evaporated, and dissolved in C/M (9:1).

4.4. Mass spectrometry

The glycosylated products were subjected to LC–MS as described previously.[43] Briefly, mass spectrometric analyses were performed using electrospray ionization (ESI)/an ion trap type mass spectrometer (Esquire 3000 plus, Bruker Daltonics, USA), coupled online by the Agilent 1100 series LC system (Agilent Technologies, USA) with ion extraction, separation, and detection in both the positive and the negative ion modes. The glycosylated products were loaded onto a 2 mm × 150 mm UK-silica column (imtakt, Japan) equilibrated with solvent A [chloroform/methanol/water (C/M/W) containing 50 mM TEA acetate buffer, pH 4.2 (83/16/1, v/v/v)] and eluted with a 0–100% linear gradient of solvent B [M/W containing 50 mM TEA acetate buffer, pH 4.2, (3/1, v/v)] in 45 min at a flow rate of 100 μL/min. The ESI parameters were as follows: nebulizer, 10.0 psi; dry gas (N_2), 4.0 L/min; dry temperature, 250 °C; negative ion mode. The mass recorded ranged from 150 to 3000 *m*/*z*.

4.5. Cell viability assay

FBJ-S1 cells (1.5×10^4) or CHO cells (3×10^3) in a 96-well microplate were incubated with 50 μM Xyl-Ser-C12 or 50 μM Xyl-pNP for 48 h. Cells treated with an equal volume of DMSO served as a negative control. Ten microliters of WST-1 dye solution (10 mM WST-1 and 0.2 mM 1-methoxy PMS, Dojindo Laboratories) per well was added to each well. After 3 h, absorbance at 450 nm with a reference wavelength of 690 nm was measured using a microplate reader (Multiskan, Labsystem).

4.6. Glycosidase digestion of glycosylated products

Glycosidase digestion of glycosylated products was carried out in 100 mM phosphate buffer (pH 7.2) containing β-galactosidase (100 U, Wako, E.C. 3.2.1.23); 50 mM sodium acetate buffer (pH 7.0) containing 5 mM calcium acetate and heparitinase (1 mU, Seikagaku, E.C. 4.2.2.8); 50 mM sodium citrate buffer (pH 5.0) containing β-*N*-acetylhexosaminidase (100 mU, Seikagaku, 100094, E.C. 3.2.1.52); 50 mM sodium citrate buffer (pH 4.3) containing α-*N*-acetylgalactosaminidase (100 mU, Seikagaku, 100086, E.C. 3.2.1.30); 20 mM phosphate buffer (pH 6.5) containing β-Glucuronidase (100 mU, Wako, 075-04631, E.C. 3.2.1.31); and 50 mM sodium phosphate buffer (pH 6.0) containing α2-3 neuraminidase (15 mU, Sigma, N7271, E.C. 3.2.1.1.8). The samples were recovered with a Sep-Pak C18 column and subjected to LC–MS/MS. Peak areas of extracted ion chromatograms of the indicated products treated with enzyme were measured, and compared with those without the enzyme treatment. The validity of enzymatic cleavage was confirmed with a positive control.

Acknowledgements

We thank Professor Tatsuya Yamagata for kindly providing FBJ-S1 cells and valuable discussions. This work was partly supported by the Global COE Project "Global COE for Human Metabolomic Systems Biology" (YW) from the Ministry of Education, Culture, Sports, Science and Technology and a Grant-in-aid for Challenging and Exploratory Research (2265108, TS) from the Japan Society for the Promotion of Science.

Supplementary data

Supplementary data associated with this article can be found, in the online version, at http://dx.doi.org/10.1016/j.carres.2012.08.003.

References

1. Varki, A. *Glycobiology* **1993**, *3*, 97–130.
2. Seeberger, P. H.; Werz, D. B. *Nature* **2007**, *446*, 1046–1051.
3. Nakajima, H.; Miura, Y.; Yamagata, T. *J. Biochem.* **1998**, *124*, 148–156.
4. Miura, Y.; Yamagata, T. *Biochem. Biophys. Res. Commun.* **1997**, *241*, 698–703.
5. Miura, Y.; Arai, T.; Yamagata, T. *Carbohydr. Res.* **1996**, *289*, 193–199.
6. Sato, T.; Takashiba, M.; Hayashi, R.; Zhu, X.; Yamagata, T. *Carbohydr. Res.* **2008**, *343*, 831–838.

7. Kasuya, M. C. Z.; Wang, L. X.; Lee, Y. C.; Mitsuki, M.; Nakajima, H.; Miura, Y.; Sato, T.; Hatanaka, K.; Yamagata, S.; Yamagata, T. *Carbohydr. Res.* **2000**, *329*, 755–763.
8. Handel, T. M.; Johnson, Z.; Crown, S. E.; Lau, E. K.; Proudfoot, A. E. *Annu. Rev. Biochem.* **2005**, *74*, 385–410.
9. Bernfield, M.; Gotte, M.; Park, P. W.; Reizes, O.; Fitzgerald, M. L.; Lincecum, J.; Zako, M. *Annu. Rev. Biochem.* **1999**, *68*, 729–777.
10. Prydz, K.; Dalen, K. T. *J. Cell Sci.* **2000**, *113*(Pt 2), 193–205.
11. Schwartz, N. B.; Galligani, L.; Ho, P. L.; Dorfman, A. *Proc. Natl. Acad. Sci. U. S. A.* **1974**, *71*, 4047–4051.
12. Okayama, M.; Kimata, K.; Suzuki, S. *J. Biochem.* **1973**, *74*, 1069–1073.
13. Izumi, J.; Takagaki, K.; Nakamura, T.; Shibata, S.; Kojima, K.; Kato, I.; Endo, M. *J. Biochem.* **1994**, *116*, 524–529.
14. Lugemwa, F. N.; Esko, J. D. *J. Biol. Chem.* **1991**, *266*, 6674–6677.
15. Siegbahn, A.; Aili, U.; Ochocinska, A.; Olofsson, M.; Ronnols, J.; Mani, K.; Widmalm, G.; Ellervik, U. *Bioorg. Med. Chem.* **2011**, *19*, 4114–4126.
16. Mani, K.; Belting, M.; Ellervik, U.; Falk, N.; Svensson, G.; Sandgren, S.; Cheng, F.; Fransson, L. A. *Glycobiology* **2004**, *14*, 387–397.
17. Mani, K.; Havsmark, B.; Persson, S.; Kaneda, Y.; Yamamoto, H.; Sakurai, K.; Ashikari, S.; Habuchi, H.; Suzuki, S.; Kimata, K.; Malmstrom, A.; Westergren-Thorsson, G.; Fransson, L. A. *Cancer Res.* **1998**, *58*, 1099–1104.
18. Garud, D. R.; Tran, V. M.; Victor, X. V.; Koketsu, M.; Kuberan, B. *J. Biol. Chem.* **2008**, *283*, 28881–28887.
19. Hyuga, S.; Yamagata, S.; Tai, T.; Yamagata, T. *Biochem. Biophys. Res. Commun.* **1997**, *231*, 340–343.
20. Yamagata, S.; Miwa, M.; Tanaka, K.; Yamagata, T. *Biochem. Biophys. Res. Commun.* **1982**, *105*, 1208–1214.
21. Salimath, P. V.; Spiro, R. C.; Freeze, H. H. *J. Biol. Chem.* **1995**, *270*, 9164–9168.
22. Freeze, H. H.; Sampath, D.; Varki, A. *J. Biol. Chem.* **1993**, *268*, 1618–1627.
23. Sato, T.; Hatanaka, K.; Hashimoto, H.; Yamagata, T. *Trends Glycosci. Glyc.* **2007**, *19*, 1–17.
24. Fritz, T. A.; Lugemwa, F. N.; Sarkar, A. K.; Esko, J. D. *J. Biol. Chem.* **1994**, *269*, 300–307.
25. Miura, Y.; Freeze, H. H. *Glycobiology* **1998**, *8*, 813–819.
26. Takagaki, K.; Nakamura, T.; Shibata, S.; Higuchi, T.; Endo, M. *J. Biochem.* **1996**, *119*, 697–702.
27. Takagaki, K.; Nakamura, T.; Kon, A.; Tamura, S.; Endo, M. *J. Biochem.* **1991**, *109*, 514–519.
28. Etchison, J. R.; Srikrishna, G.; Freeze, H. H. *J. Biol. Chem.* **1995**, *270*, 756–764.
29. Kitagawa, H.; Kano, Y.; Shimakawa, H.; Goto, F.; Ogawa, T.; Okabe, H.; Sugahara, K. *Glycobiology* **1999**, *9*, 697–703.
30. Kitagawa, H.; Shimakawa, H.; Sugahara, K. *J. Biol. Chem.* **1999**, *274*, 13933–13937.
31. Tone, Y.; Pedersen, L. C.; Yamamoto, T.; Izumikawa, T.; Kitagawa, H.; Nishihara, J.; Tamura, J.; Negishi, M.; Sugahara, K. *J. Biol. Chem.* **2008**, *283*, 16801–16807.
32. Sugahara, K.; Kitagawa, H. *Curr. Opin. Struct. Biol.* **2000**, *10*, 518–527.
33. Stow, J. L.; Farquhar, M. G. *J. Cell Biol.* **1987**, *105*, 529–539.
34. Basappa; Murugan, S.; Sugahara, K. N.; Lee, C. M.; ten Dam, G. B.; van Kuppevelt, T. H.; Miyasaka, M.; Yamada, S.; Sugahara, K. *Glycobiology* **2009**, *19*, 735–742.
35. Sato, T.; Fujita, S.; Kasuya, M. C. Z.; Hatanaka, K.; Yamagata, T. *Chem. Lett.* **2004**, *33*, 580–581.
36. Gruzman, A.; Shamni, O.; Ben Yakir, M.; Sandovski, D.; Elgart, A.; Alpert, E.; Cohen, G.; Hoffman, A.; Katzhendler, Y.; Cerasi, E.; Sasson, S. *J. Med. Chem.* **2008**, *51*, 8096–8108.
37. Utille, J.-P.; Gagnaire, D. *Carbohydr. Res.* **1982**, *106*, 43–57.
38. Rowell, R. M.; Feather, M. S. *Carbohydr. Res.* **1967**, *4*, 486–491.
39. Johnsson, R.; Ellervik, U. *Synlett* **2005**, 2939–2940.
40. Mori, M.; Ito, Y.; Ogawa, T. *Carbohydr. Res.* **1990**, *195*, 199–224.
41. Yamagata, S.; Tanaka, R.; Ito, Y.; Shimizu, S. *Biochem. Biophys. Res. Commun.* **1989**, *158*, 228–234.
42. Wang, L.; Takaku, S.; Wang, P.; Hu, D.; Hyuga, S.; Sato, T.; Yamagata, S.; Yamagata, T. *Glycoconj. J.* **2006**, *23*, 303–315.
43. Ogasawara, N.; Katagiri, Y. U.; Kiyokawa, N.; Kaneko, T.; Sato, B.; Nakajima, H.; Miyagawa, Y.; Kushi, Y.; Ishida, H.; Kiso, M.; Okita, H.; Sato, T.; Fujimoto, J. *J. Biochem.* **2011**, *149*, 321–330.